WHOLE BODY KINEMATICS USING POST MORTEM HUMAN SUBJECTS IN EXPERIMENTAL REAR IMPACT

M.Philippens, J.Wismans, H.Cappon

TNO Crash Safety Centre

N.Yoganandan, F.Pintar

Medical College of Wisconsin

ABSTRACT

This research was initiated to create an accurate dataset with respect to the kinematics of 5th and 95th percentile human subjects under low and moderate rear end impact conditions. For this purpose, rigid seat rear impact sled experiments were conducted using 5 unembalmed Post Mortem Human Subjects (PMHS): four 5th percentile females and one 95th percentile male restrained with a three-point belt. The sled velocity changes were 16 and 25 km/hr, sled accelerations were 3 to 5 g. Photographic targets attached to the head, T1 and pelvis were filmed at 1000 f/sec. The subjects were instrumented with tri-axial accelerometers on the head, T1 and pelvis, and a tri-axial angular velocity sensor on the head. A post-test physical examination was conducted showing injuries in two subjects. Kinematics of head, T1 and pelvis and the loads at occipital condyles and T1 level will be presented. Data can be used in the development of human mathematical models and the design of rear impact crash dummies. The data presented here can be used in addition to numerous data on human subjects, mainly volunteers at low Δ V's. The differences between the 5th and 95th percentile subjects appear to indicate the need to validate any human surrogate in relation to its body size.

KEYWORDS

BIOMECHANICS, CADAVERS, REAR IMPACTS, KINEMATICS

THE MOST CITED experiments, on human neck impact response are the hyperextension tests performed by Mertz and Patrick (1967). However T1 kinematics were not incorporated in these results, therefore, head-neck kinematics could not be separated from motion from the thoracic and lumbar spine. The same authors presented a head angle moment of force corridor for the neck flexion and extension later on used to design the Hybrid III neck (Mertz 1971). At the Japan Automobile Research Institute (JARI), a number of sled experiments with volunteers have been performed (Ono, 1993, 1997a, 1997b). Head accelerations were monitored and the motion of the head recorded with high-speed video. In the latest series of experiments at JARI, the motion of the cervical vertebras was recorded by high speed X-ray (Ono 1997a, 1997b). An extensive study was performed by Siegmund (1997). He exposed 21 males and 21 females to vehicle impacts. Kinematic data were obtained for the

head, the C7-T1 joint axis in a global reference frame, and head kinematic data relative to the C7-T1 joint axis. Rotation of the co-ordinate frame originating at C7-T1 was obtained from the rotation of the torso. Neck loads were not calculated. Kinematics and dynamics of the head neck, including neck loads, as found in volunteer sled tests were presented by van den Kroonenberg (1998). The subjects were seated in a modern car seat with headrest. It was indicated that there is a difference in the kinematic response of males and females. Ono (1999) presented data on human volunteer rear impact responses, where unique data on the deformation of the spine and the pressure distribution of the back were presented. The loading level in previous work is relatively low due to the use of human volunteers. And the use of real car seats is a disadvantage to create well-defined conditions required for validating human models. One reference was found where PMHS rear end tests at a high loading level, 7g, were performed (Kallieris 1996). However, this research was not focussed on the kinematic response, but analysed the neck loads with respect to the injuries found. Geigl (1994, 1995) compared the responses of PMHS to volunteer responses, at Δ V's of 6 and 15 km/hr and 3 to 6 g. Davidsson (1998) published responses of volunteers at low non-injurious loading levels. The work presented here is meant to be conducted in injury causing loading ranges.

The aim of this research is to generate a PMHS data set to be used for validation of numerical and mechanical human models in addition to the previous work described above. Kinematic responses are generated using four 5th and one 95th P(ost)M(ortem)H(uman)S(ubjects) in rigid seat rear impact loading conditions. The tests are performed in collaboration with the medical College of Wisconsin. The response of the subjects will be presented. The maximum head-neck loads at the occipital condyles and T1 level and anthropometric data as well as summary of the autopsy findings are included.

MATERIAL AND METHODS

TEST PROGRAM Tests were performed at two nominal ΔV's: 16 and 25 km/hr, which represent respectively a mid- and high- severe loading level for low velocity rear impacts, as most neck injuries in rear-end collisions were found for ΔV's of less than 20 km/hr (Thunnissen, 1996;Temming, 1998). For each ΔV a test with and without upholstery attached to the rigid seat back panel was performed with a 5th percentile female PMHS (four tests in total). A fifth test was performed with a 95th male subject at 25 km/hr back panel upholstery. Characteristics of the upholstery are included in Appendix B. The test matrix is presented in Table 1.

Table 1: Specification of actual test conditions

Test No	Subject identifier	%-tile	Length [m]	Weight [kg]	ΔV [km/hr]	Average sled acc. [g]	Back panel upholstery
1	RIPMHS102	5	1.56	55.4	14.9	3.3	No
2	RIPMHS103	5	1.65	40.4	15.9	3.3	Yes
3	RIPMHS101	5	1.64	72.6	24.8	4.6	No
4	RIPMHS105	5	1.52	36.3	24.5	4.7	Yes
5	RIPMHS104	95	1.85	107.5	23.7	4.4	Yes

ANTHROPOMETRY The anthropometry of the subjects is documented in Appendix A.

TEST SET UP

Sled configuration A rigid steel seat is mounted on the sled (Figure 1) with the seat panel inclined 10 degrees upward and the back panel inclined 25 degrees backwards. A drawing with dimensions of

the seat is presented in Appendix B. A lateral view of the seat is presented in Figure 2. Two slots at the top and bottom of the back panel provide space for the instrumentation and photo targets mounted at the back of the subject. The sled accelerations are presented in Figure 6. The negative acceleration after approximately 150 ms is caused by the braking system of the sled. This is quite prominent for the first test, 25 km/hr-5% rigid seat but is reduced for the remaining four tests.

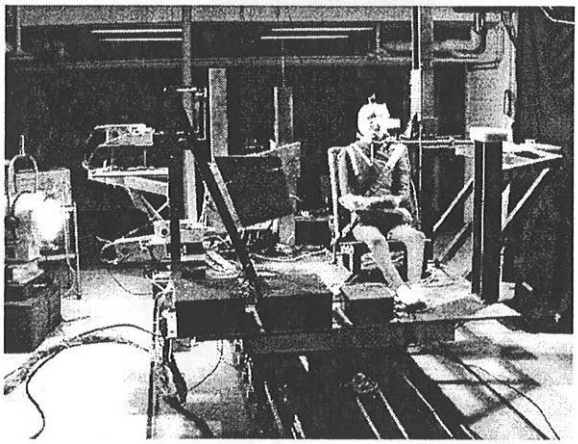

Figure 1: Test set-up at Medical College of Wisconsin

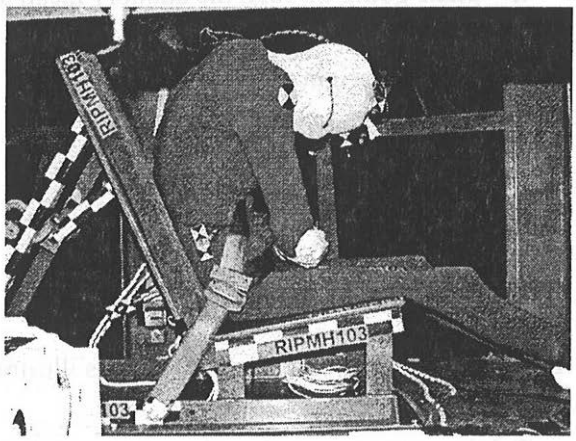

Figure 2: The rigid seat

Subject positioning The subject is positioned on the seat with the Frankfort plane horizontally and restrained by a three point belt with retractor. Position of the anchorage points and length of the shoulder and lap section of the belt are documented for each test, (Appendix B). The lap section of the belt is locked after being hand tightened, to prevent extreme whole body upward motion. A special designed device stabilises the initial position of the head. This device moves out of the rebound area propelled by g-forces. The head is positioned carefully on the support and immediately lifts off this support at initial deceleration of the sled. The arms are positioned in front of the thorax and taped together to prevent them covering the field of view of the cameras. This also provides a more controlled motion of the subject.

Instrumentation Electromechanical sensors were mounted externally to the subjects' head, T1 and pelvis. Linear acceleration of head, T1 and pelvis were measured and additionally the angular velocity of the head. Photo targets attached to the instrumentation mounting bases are used to calculate the kinematics of anatomical defined co-ordinate systems of head, T1 and pelvis. Two film cameras, running at 1000 f/sec are set up to record a detailed view of the head-upper torso and upper torso-pelvis. Both views are partially overlapping. The linear acceleration of the sled and the belt forces in the lap and shoulder section are measured.

DATA PROCESSING AND ANALYSIS METHOD The general method to analyse the response of the Post Mortem Human subjects in human head-neck tests is described by Wismans (1986). Van den Kroonenberg (1998) presented an updated method used for volunteer tests. Details on the test and data processing methodology are described in Yoganandan (2000). The responses of the subject are characterised by the kinematics of the head and T1. In addition to these also the kinematics of the pelvis are required for the tests reported here, as the responses will be extended to the overall spine responses.

Anatomical co-ordinate systems Anatomical landmarks define the anatomical co-ordinate systems. The anatomical landmarks of head and pelvis are marked with small steel balls prior to the tests. These landmarks are visible on the pre- and post-test x-rays. The spinous process of T1 is marked also by a steel ball. The anterior superior edge of the T1 vertebral body is detected visually from the x-rays.

Head

The anatomical co-ordinate system is illustrated in Figure 3.

Origin: middle between left and right auditory meatus

x-y plane going through the auditory meati and infra-orbital notches

x-axis: from origin to anterior

y-axis: along line connecting auditory meati, from right to left

z-axis: caudal-cranial

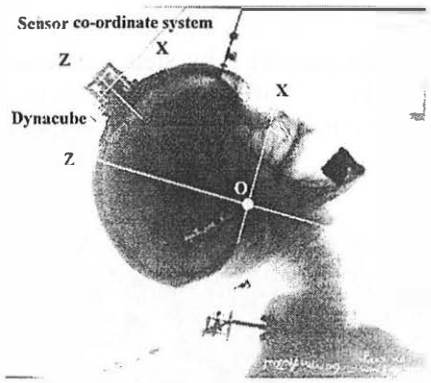

Figure 3: Head anatomical co-ordinate system

T1

The T1 anatomical co-ordinate system is illustrated in Figure 4.

Origin: anterior superior edge of T1 vertebral body

x-axis: posterior edge of spinous process to origin

y-axis: perpendicular to x-z axis, right to left

z- axis: perpendicular to x-axis in midsagital plane, caudal cranial

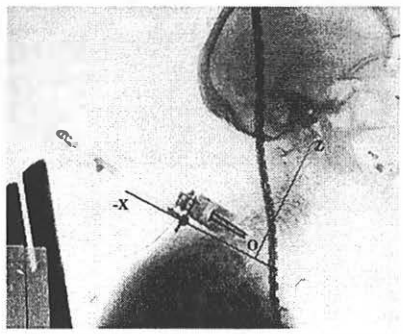

Figure 4: T1 anatomical co-ordinate system

Pelvis

The pelvis anatomical co-ordinate system is illustrated in Figure 5.

Origin: Pubic Symphysis

x- axis: perpendicular to z-axis in mid sagital plane

y- axis: perpendicular to x-z axis, right to left

z-axis: pubic symphysis to middle of spinae iliaca anterior superior

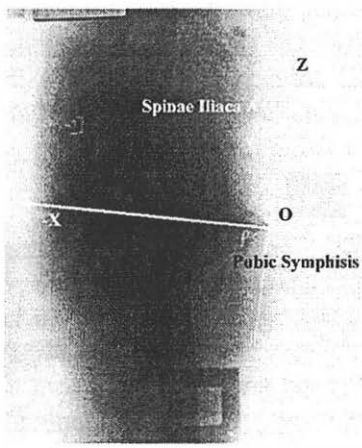

Figure 5: Pelvis anatomical co-ordinate system

Head Inertial and Geometric Properties The inertial properties of the head, mass and moment of inertia about the y-axis needed to calculate the neck loads. They are calculated by a regression formula developed by McConville (1980) and based on specific dimensions of the head.

The position of the head CG w.r.t. the anatomical co-ordinate system is a value based on Beier (1980) as used by Wismans (1986); CG: x:8.3 mm y:0 mm z:31 mm.

The occipital condyle co-ordinates obtained from the x-rays are specified in Table 2.

Table 2: Anatomical co-ordinates of the occipital condyles derived from X-rays

PMHS	x [mm]	z [mm]
101	-3	-22
102	-10	-16
103	-12	-6
104	5	-22
105	2	-7

The OC co-ordinates of specimen 101 are within the range as published by Ewing (1973): average x: -11 mm, z: -26 mm. Subject 102,103 and 105 show a smaller z-co-ordinate compared to the range specified by Ewing. Subjects 104 and 105 have a positive x co-ordinate. Which means that the OC is anterior to the anatomical origin. X co-ordinates published by Ewing are less than -5 mm. It is not known to what extent the body dimensions of the PMHS are comparable to the specimens used by Ewing.

Kinematics The co-ordinates of the photo targets attached to the different body segments are obtained by digitising the high-speed films. The position and orientation of the segment anatomical co-ordinate systems are calculated relative to a sled based coupled co-ordinate system. Then the relative motion of head w.r.t T1, T1 w.r.t pelvis are determined. Motion of the pelvis w.r.t. the sled is implicitly known from the basic data set. Out of plane motions (y co-ordinate) are found to be small so they will be neglected here further. Consequently the motion of the head is specified by the x(t), z(t) co-ordinates of the occipital condyles and the angular position of the head. T1 kinematics are specified by the x(t), z(t) co-ordinates of T1 anatomical origin and the angular orientation of T1 co-ordinate system, and the pelvis motion is specified similarly.

OC and T1 loads Loads at OC and T1 level are calculated using the measured linear and angular acceleration of the head, the kinematics and inertial properties. The equations for these calculations are presented in Appendix C. The maximum shear force (Fx), tension force (Fz) and bending moment (My) at OC and T1 will be presented, where the effect of the neck mass is neglected.

RESULTS

KINEMATIC RESPONSES Time histories of the head displacements relative to T1, of T1 relative to the pelvis and of the pelvis relative to the sled are presented in Figs. 8-10, 11-13, 14-16, respectively. Moreover in Appendix D time histories of the head and T1 relative to the sled are presented. At t=0 the initial values of the co-ordinates all are set to zero in order to make an easier comparison possible of the results. In Fig 16 and 17 the trajectories of the head cg and occipital condyles relative to T1 origin are expressed (in a co-ordinate system aligned with the sled).

The following observations can be made. The head initially starts to translate relative to the sled while the head rotation almost remains zero. Together with the translation of the head also T1 starts rotating. This head-neck motion is often referred to as head-lag and is also observed in frontal impacts. It is thought to be of importance in the development of a mechanical or mathematical model of the head-neck system. In one test (i.e. 25 km/h,, 5% u) this head lag was less present. No explanation for this can be given. Maximum head rotations (relative to the sled) in all test were of the same order of magnitude (120-150 degrees) except for test 25 km/h, 5% r, where a non-fixed belt was used (for details see test set-up). If we look to the relative head rotations (relative to T1) it can be noticed that in the tests were the head lag is present first a positive rotation of about 40 degrees takes place followed by a negative (backward) rotation of about 50 degrees. In the test without a fixed belt the relative rotation is much larger: (about 90 degrees). The T1 translations relative to the sled (see Appendix D) show a backward translation of about 15 cm and an upward displacement of about 6 cm except for the test with the 95th percentile subject, which exhibits a backward translation and upward translation about twice as high. So this clearly shows a subject dependency. Moreover a dependency of the test velocity and the type of belt fixture can be observed.
If we consider the vertical displacement of T1 relative to the pelvis it can be seen that in 2 of the tests a stretching of about 10 cm occurs and in one test of about 4 cm (in the 2 other tests this quantity could not be determined because of film target contact).

The vertical displacement of the pelvis in the 5th perc. upholstery test is small compared to both other subjects. The 95th subject shows a large T1 rotation. The head touching the T1 targets and pushing them down causes the sudden increase of the T1 angle, at 0.2 seconds for the 5th percentile subject with back panel upholstery. The motion of the pelvis is significantly larger for the 95th percentile subjects. This is probably caused by the corpulence of this subject. The 5th percentile subjects, in the other hand, were extremely slim around pelvis and upper legs.

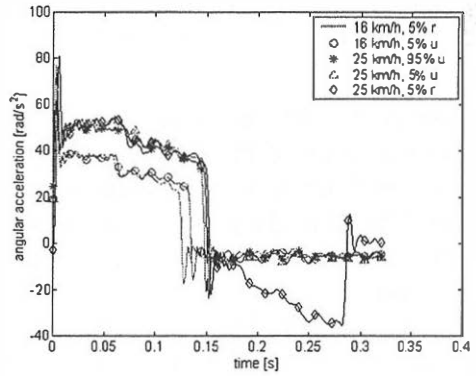

Figure 6: Sled pulse

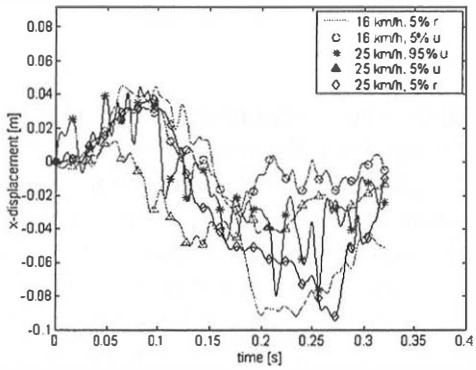

Figure 7: x-displacement of the occipital condyle with respect to T1

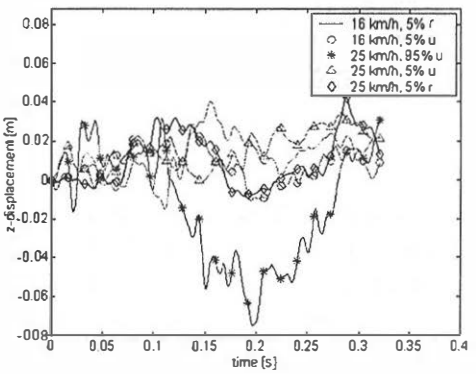

Figure 8: z-displacement of the occipital condyle with respect to T1

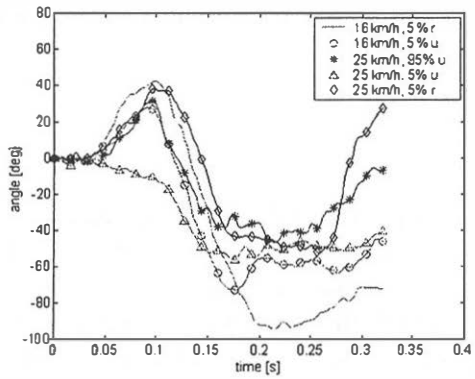

Figure 9: Head angle with respect to T1

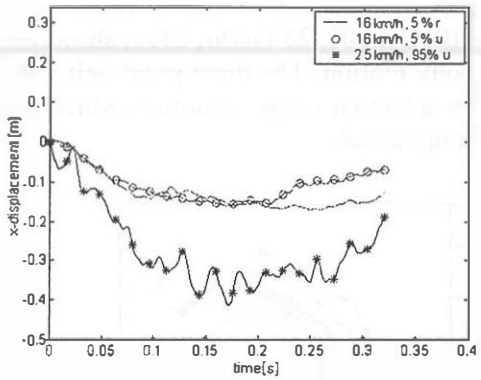

Figure 11: x-displacement of the T1 anatomical origin with respect to the pelvis

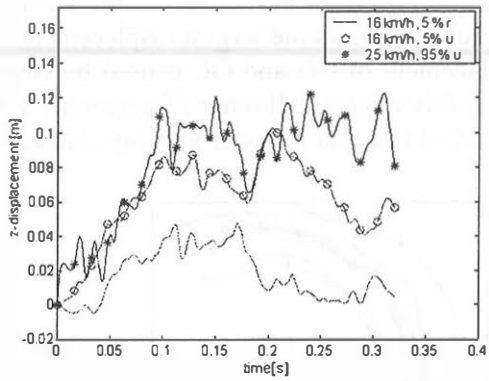

Figure 10: z-displacement of the T1 anatomical origin with respect to the pelvis

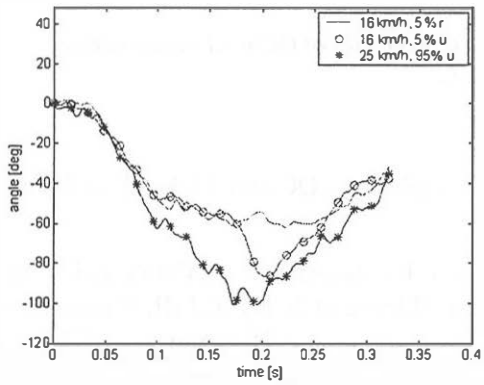

Figure 12: T1 angle with respect to the pelvis

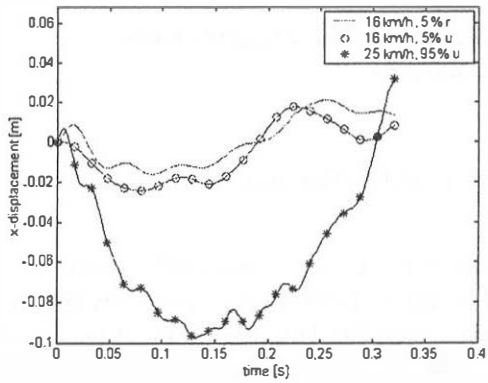

Figure 13: x-displacement of the pelvis anatomical origin with respect to the sled

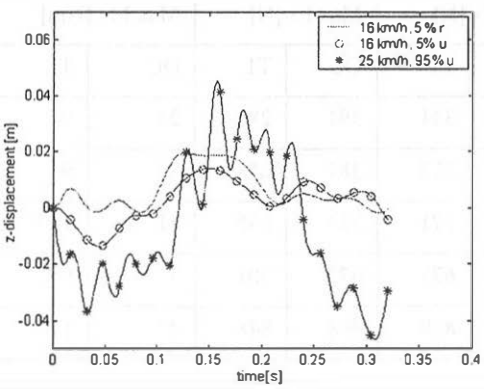

Figure 14: z-displacement of the pelvis anatomical origin with respect to the sled

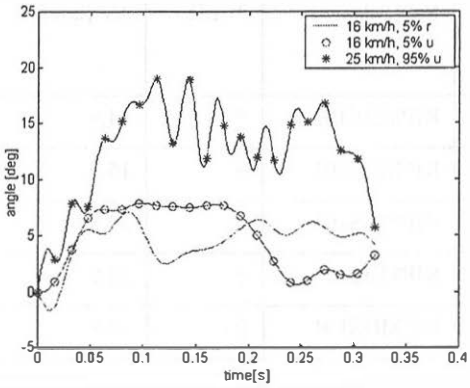

Figure 15: Pelvis angle with respect to the sled

The trajectories of CG and OC with respect to a non-rotating T1 are presented in Figure 16 and Figure 17. A distinct horizontal translation of the head at the initial phase of the motion is seen. The 95th percentile subject shows the largest displacement. Subject RIPMHS101, 25 km/hr, 5% r, shows also a large displacement of CG and OC caused by large whole body motion. The three-point belt was not clamped for this subject. All other 5th percentile subjects show a similar range of motion, which means that no effect of the upholstery or velocity change can be distinguished.

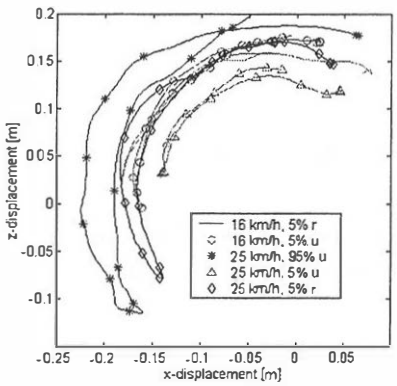

Figure 16 Trajectories of head CG w.r.t. non rotating T1

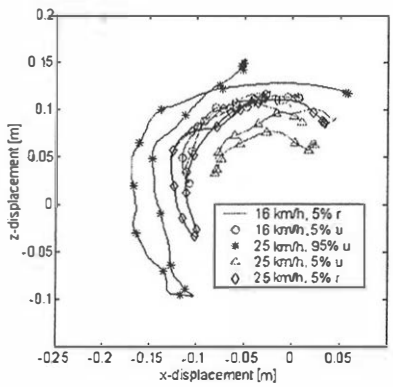

Figure 17 Trajectories of OC w.r.t. non rotating T1

OC AND T1 LOADS The maximum loads during the extension phase at OC and T1 level are listed in Table 3.

The OC tension forces are significantly lower than the tolerance levels (AIS ≥3), 2470 N and 4730 N as reported by Mertz (1997) for respectively the small female and large male Hybrid III. The tolerance levels for the extension bending moment specified by the same author are 38.7 Nm and 102.7 Nm. Only subject RIPMHS101 exceeds this value. The bending moment for the 95th percentile subject is half the tolerance level.

Table 3 Maximum loads at occipital condyle and T1 level

Test No	Subj. id	%-tile	ΔV [km/hr]	Max Fx [N]		Max Fz [N]		Max My [Nm]	
				OC	T1	OC	T1	OC	T1
1	RIPMHS102	5	14.9	398	331	391	281	24	94
2	RIPMHS103	5	15.9	387	372	387	258	33	97
3	RIPMHS101	5	24.8	401	571	734	638	41	100
4*)	RIPMHS105	5	24.5	180	675	672	501	32	90
5	RIPMHS104	95	23.7	536	809	908	848	47	130

*) Head touched back panel just before maximum extension

AUTOPSY RESULTS

Injuries as identified by x-rays and CT scans were as follows. For RIPMHS 104 C5-C6 anterior distraction and for RIPMHS 105 anterior chip fracture of C5 vertebral body. No other injuries were identified in other specimens. More detailed injuries are found based on cryo-microtome autopsy.

Analysis of these findings, including the dynamic responses e.g.: accelerations and loads is still in progress.

DISCUSSION AND CONCLUSIONS

In general it can be concluded that the data have sufficient quality to generate a data set to be used for evaluation of human numerical models and mechanical human surrogates. For some tests contact between head and the T1 target mount scattered the results for part of the motion. A similar artefact occurred for the pelvis target mount, which was disturbed by contact with the seat back panel. Optimisation of the T1 photo target bracket did reduce the risk of contact between head and T1 targets.

The use of a fixed belt in test 2-5 showed a less extreme motion of the subjects compared to test1. Which appears to be more realistic related to the standard automotive test condition and probably will improve the reproducibility and consistency of the data.

The data presented here have an improved quality with respect results of volunteer tests. Detailed kinematics can be obtained as the instrumentation is directly mounted to the bony structures. And the position of the instrumentation with respect to the underlying anatomical structure can be obtained by the use of X-rays. The use of X-rays is very limited or not always possible in volunteer tests due to ethical restrictions. PMHS tests allow greater head-neck excursions and larger loading levels compared to volunteer tests. The absence of muscle activity in PMHS will result in a different response compared to living human subjects. However this becomes more important in the rebound phase.

The following conclusions can be made:

- The restraint system has a significant effect on the kinematics of the subjects. A standard three-point belt, which was not clamped, allows for larger whole body motions. The rigid seat without head restraint appears to induce a significant backward rotation of the upper body resulting in a significant upward motion of the pelvis. A fixed belt ensures a more restricted response of the subject.
- The impact severity and the size of the subject does not significantly affect the horizontal displacement of T1
- The results give no clear indication of a relation between the impact severity and the maximum absolute rotation of T1.
- The absolute x and z displacement of the head appear to be more affected by the size of the subject than by the impact severity. Especially the z displacement increases for a larger subject. This is prominently visible in figures 24 and 25, Appendix D. Especially when the 25km/hr, 5^{th} percentile rigid seat test is omitted. The subject showed large excursions due to the use of a 3 point belt with a non-fixed lap section.
- The vertical displacement of T1 with respect to the sled is slightly larger in the 25 km/hr test compared to the vertical displacement found in the 16 km/hr test.
- The thickness of the upholstery seems to be distinguishable in the pelvis horizontal displacement. The pelvis x displacement is about 0.01 m larger for the test with upholstery compared to the test without.
- No significant difference in the horizontal displacement of T1 with respect to the pelvis is seen between the tests with and without upholstery.

It should be noted that the conclusions made with respect to the subject response can not be generalised, as the number of tests is limited. The results for these 5th and 95th percentile subjects can be used in addition to the numerous data from other authors, described in the introduction. These are mainly related to volunteers which consequently limits the ΔV. And the use of real car seats limits the use for validation of a human model as the characteristics of the seat have a significant effect on the response of the subject. The observed differences between the 5th and 95th percentile subjects appear to confirm the necessity to validate any human surrogate in relation to its body size.

ACKNOWLEDGEMENT

This research program was initiated by a consortium composed of Ford Motor Company, Lear Corporation, Breed Technologies and TNO Crash Safety Centre. The research at Medical College of Wisconsin was supported in part by R49CCR515433 and VA Medical Research.

REFERENCES

Beier G., Schuck M., Schuller E., Spann W.: Determination of physical data of the head. I. Centre of gravity and moments of Inertia of human heads. IRCOBI 1980

Davidsson J., Deutscher C., Hell W., Linder A., Lövsund P., Svensson M.Y.: Human Volunteer Kinematics in Rear-End Sled Collisions, IRCOBI 1998, pg 289-301.

Ewing C.L., Thomas D.J.: Torque versus Angular Displacement Response of Human Head to –Gx Impact Acceleration. 17th Stapp Car Crash Conference, 1976, SAE 730976.

Geigl B.C., Steffan H., Leinzinger P., Roll, Mühlbauer M., Bauer G.: The Movement of the Head and Cervical Spine During Rear-end Impact, IRCOBI, 1994, pg 127-137.

Geigl B.C. Steffan H., Dippel Ch., Muser M.H., Walz F., Svensson M.Y.: Comparison of Head-Neck Kinematics during Rear End Impact between Standard Hybrid III, RID Neck, Volunteers and PMTO's, IRCOBI, 1995, pg 261-270.

van den Kroonenberg A., Philippens M., Cappon H., Wismans J., Hell W., Langwieder K.: Human Head-Neck Response during Low-Speed Rear End Impacts.42nd Stapp Car Crash Conference, 1998.

McConville J.T., Churchill T.D., Kaleps I., Clauser C.E., Cuzzi J.: Anthropometric Relationships of Body and Body Segment Moments of Inertia. AFAMRL-TR-80-119, Air Force Medical Research Laboratory, Aerospace Medical Division, Air Force Systems Command, Wright-Patterson Air Force Base, Ohio 45433, 1980.

Mertz H.J., Patrick L.M.: Investigations of the Kinematics and Kinetics of Whiplash. 11th Stapp Car Crash Conference, SAE 670919, 1967

Mertz H.J., Patrick L.M.: Strength and Response of the Human Neck. 15th Stapp Car Crash Conference, SAE 710855, 1971.

Mertz H.J., Prasad P., Irwin A.L.: Injury Risk Curves for Children and Adults in Frontal and Rear Collisions, 41st Stapp Car Crash Conference, SAE 973318, P-315, 1997

Ono K., Kanno M.: Influence of the physical Parameters on the risk to Neck Injuries in low Impact Speed Rear-End Collisions. IRCOBI, 1993

Ono K., Kaneoka K.: Motion analysis of human cervical vertebrae during low speed rear impacts by the simulated sled. Int. IRCOBI, 1997a

Ono K., Kaneoka K., Kajzer J., Wittek: A: Cervical Injury Mechanism Based on the Analysis of Human Cervical Vertebral Motion and Head-Neck-Torso Kinematics During Low Speed Rear Impacts. 41th Stapp Car Crash, SAE 973340, 1997b

Ono K., Inami S., Kaneoka K., Gotou T., Kisanuki Y., Sakuma S., Kazuo M.: Relationship between Localized Spine Deformation and Cervical Vertebral motions for Low Speed Rear Impacts Using Human Volunteers. IRCOBI, 1999, pg 149-164.

Severy D.M., Mathewson J.H., Bechtol C.O.: Controlled automobile rear end collisions – an investigation of related engineering and medical phenomena. Canadian Services Medical Journal, pages 727-759, 1955

Siegmund G.P., King D.J., Lawrence J.M., Wheeler JB, Brault J.R, Smith T.A: Head/Neck Kinematic response of Human Subjects in Low-Speed Rear-End Collisions. 41th Stapp Car Crash Conference, SAE 973341, 1997

Temming J.: Human Factors Data in Relation to Whiplash Injuries in Rear End Collisions of Passenger Cars. SAE paper 981191, 1998

Thunnissen J.G.M., van Ratingen M.R., Beusenberg M.C., Janssen E.G.:A Dummy Neck for Low Severity Rear Impacts", 15th International Conference on Experimental Safety Vehicles, 1996.

Wismans J., van Oorschot H., Woltring H.J.: Omni-Directional Human Head-Neck Response. 30th Stapp Car Crash Conference, SAE 861893, 1986

Yoganandan N., Pintar F.A.: Frontiers in Whiplash Trauma: Clinical and Biomechanical. The Netherlands, IOS Press, 2000.

APPENDIX A

PMHS ANTHROPOMETRY: the anthropometry is documented in Table 4. The specified dimensions are illustrated in Figure 18-Figure 20.

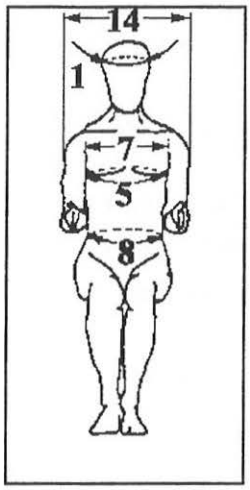

Figure 18: frontal view

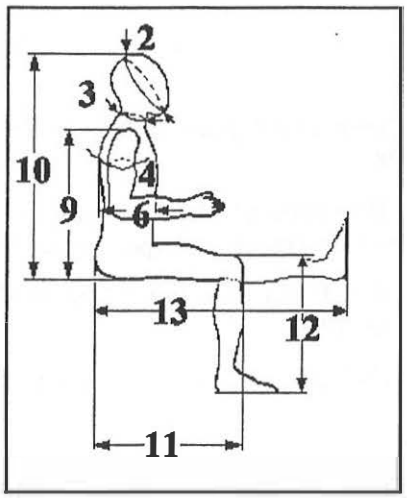

Figure 19: side view

Figure 20: head

Table 4: Anthropometric data of PMHS (all sizes in [mm])

Subject Id.	RIPMHS101	RIPMHS102	RIPMHS103	RIPMHS104	RIPMHS105
Testnumber testmatrix	4	1	2	5	4
Body weight [kg]	72.6	55.4	40.4	107.5	36.6
Body length	1638	1560	1650	1850	1625
Gender	Female	Female	Female	Male	Female
1. Hat size	559	535	560	605	540
2. Occip-chin circumf	Na[1)]	Na[1)]	Na[1)]	Na[1)]	Na[1)]
2a. Head length	181	170	190	190	175
2b. Head width	150	150	145	160	150
2c. Head height	210	200	193	240	210
3. Neck circumf.	390	280	285	435	295
4. Upper arm circumf.	290	185	180	325	160
5. Chest circumf.	970	760	740	960	675
6. Chest height	207	210	200	245	190
7. Chest width	321	245	245	320	215
8. Abdomen cicumf.	327	510	620	870	605
9. Buttock-shoulders	Na[1)]	Na[1)]	Na[1)]	Na[1)]	Na[1)]
10. Sitting height	838	820	830	1030	760
11. Pelvis-knee	523	525	560	525	535
12. Sole of foot-knee	480	445	465	525	475
13. Pelvis-heel	1003	970	1025	1050	1010
14. Shoulder width	Na[1)]	Na[1)]	Na[1)]	Na[1)]	Na[1)]

[1)] Not available

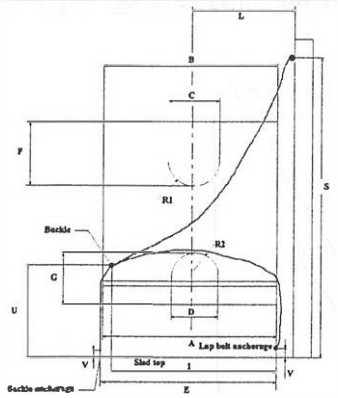

Figure 22:Specification of seat dimensions, front view

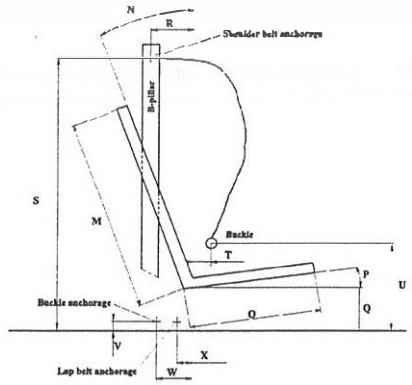

Figure 21: Specification of seat dimensions, side view

Table 5: Specification of length of belt sections

MCW test identification	Shoulder belt length [mm]	Lap belt length [mm]
RIPMH 101	Na[1)]	Na[1)]
RIPMH 102	940	790
RIPMH 103	760	690
RIPMH 104	900	965
RIPMH 105	830	775

1) Not available

Table 6: Dimensions of seat and position of belt anchorage points

Measure	Description	Size /angle [mm]/[deg]	Measure	Description	Size/angle [mm]/[deg]
A	width seat panel	448	O	Length seat panel	400
B	width back panel	448	P	Incl.. seat panel	10°
C	width top slot	128	Q	height seat	155
D	width bottom slot	130	R1	radius top slot	64
E	width lap b. anch.	Tst 101 :605 Tst 102-5 : 445	R2	radius bottom slot	65
F	length top slot	Tst 101-2-3-5: 235 Tst 104 : 199	S	height shoulder anch.	Tst 101-2-3-5:920 Tst 104 : 1037
G	length bottom slot	Tst 101-2-3-5:198 Tst 104 : 198	T	for- aft buckle	Not available
I	width buckle	Not available	U	height buckIle	Tst 104: 225
L	width should. anch.	264	V	height lap anchorage	25
M	height back panel	Tst 101-2-3-5:583 Tst 104 :700	W	for-aft buckle anch.	78
N	Inclin. back panel	24°	X	for-aft lap anch	Tst 101: 0 Tst 102-5 : 70

Upholstery attenuation characteristic

The foam is impacted with a rigid surface of 300 x 300 mm. Impacting mass 22.2 kg, impact velocity is 15.8 km/hr.

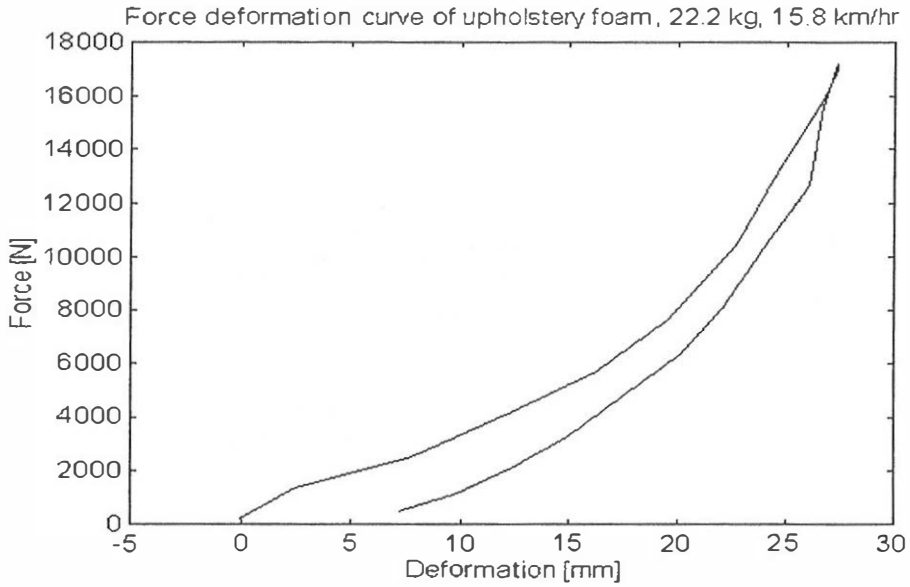

Figure 23: Load deformation curve of foam upholstery

The data are presented in the next table:

Table 7: Load deformation data of upholstery foam

Displacement [mm]	Force [N]	Displacement [mm]	Force [N]
-0.08153	208	26.6594	15619
2.52734	1372	26.0072	12674
7.74509	2537	24.0505	10276
12.3106	4181	22.0939	8085
16.2239	5687	20.1372	6372
19.485	7674	17.5284	4797
22.7461	10413	14.9195	3290
24.7028	13085	12.3106	2126
26.6594	15824	9.70174	1099
27.3116	16989	7.09287	482
27.3116	17194		

$$F_{ocx} = m_h(a_x - g\sin(\varphi))$$
$$F_{ocz} = m_h(a_z + g\cos(\varphi))$$
$$T_{ocy} = J_{cgy}\ddot{\varphi} + d_{occgz}F_{ocx} - d_{occgx}F_{ocz}$$

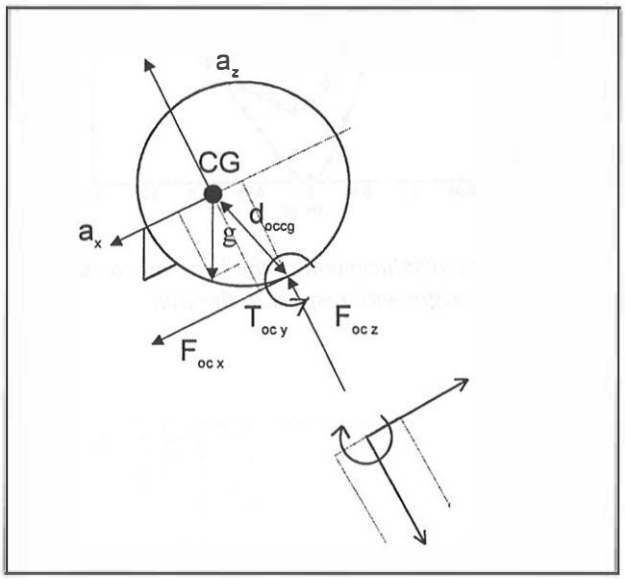

F_{ocx} = x component of force at the OC joint applied by the neck to the head

F_{ocz} = z component of force at the OC joint applied by the neck to the head

T_{ocy} = y component of torque at the OC joint applied by the neck to the head

J_{cgy} = moment of inertia of the head about the y-axis

m_h = head mass

a_x = x component of head acceleration

a_z = z component of head acceleration

φ = head angle with respect to sled frame

d_{occg} = distance between OC and head-CG

g = gravity (9.81 m/s^2)

Figure 24: Calculation of forces and torques at OC

When the neck is considered to be without mass, then similar equations hold for the neck loads at T1. The coordinate system in which these loads are expressed is the T1 coordinate system. Thus rotation of the calculated loads with head angle with respect to T1 (φ_r) is needed, resulting in the following equations:

$$F_{t1x} = F_{ocx}\cos(\varphi_r) + F_{ocz}\sin(\varphi_r)$$
$$F_{t1z} = F_{ocz}\cos(\varphi_r) - F_{ocx}\sin(\varphi_r)$$
$$T_{t1y} = J_{cgy}\ddot{\varphi} + d_{t1cgz}F_{t1x} - d_{t1cgx}F_{t1z}$$

Where

F_{t1x} = x component of force at T1 level

F_{t1z} = z component of force at T1 level

φ_r = angle between head anatomical coordinate system and T1 anatomical coordinate system.

T_{t1y} = y component of torque at T1 level applied by the neck to T1

d_{t1cgx} and d_{t1cgz} are respectively the x and z distance between head center of gravity and the T1 anatomical origin.

APPENDIX D

The x and z, and angular orientation time traces of the head, T1 anatomical co-ordinate systems with respect to a sled based co-ordinate system. All data are with respect to their initial values at t=0.

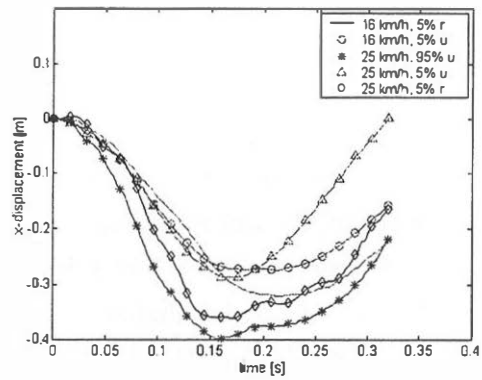

Figure 25: x-displacement of the head anatomical origin with respect to the sled

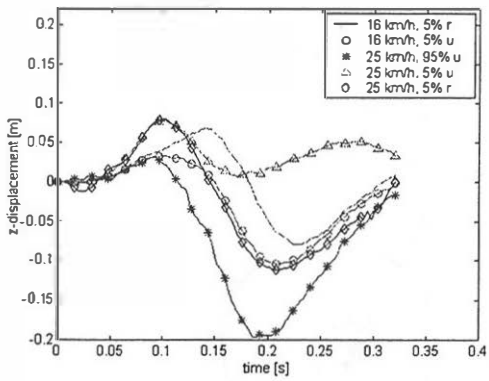

Figure 26: z-displacement of the head anatomical origin with respect to the sled

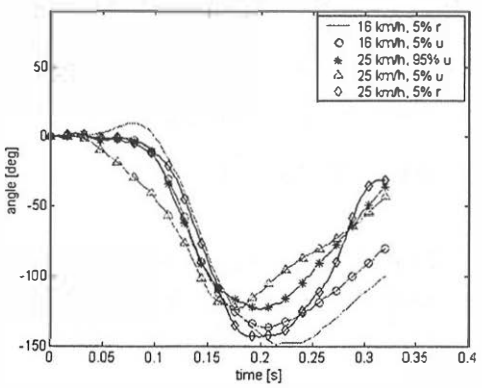

Figure 27: Head angle with respect to the sled

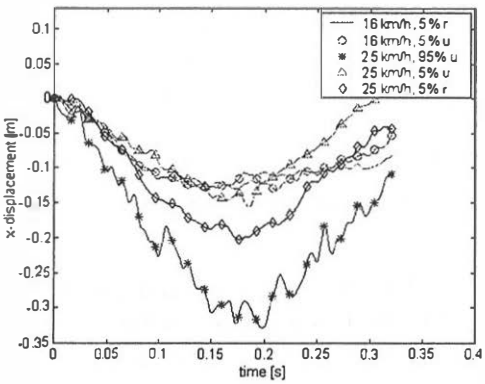

Figure 28: x-displacement of the T1 anatomical origin with respect to the sled

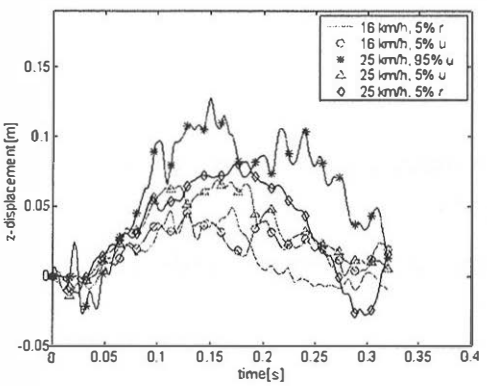

Figure 29: z-displacement of the T1 anatomical origin with respect to the sled

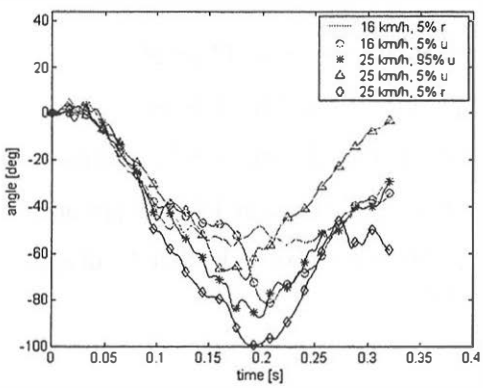

Figure 30: T1 angle with respect to the sled